Journal of Biomedical Optics 8(3), 428–431 (July 2003)

Mechanisms of membrane potential sensing with second-harmonic generation microscopy

Thomas Pons
Laurent Moreaux
ESPCI
INSERM EPI 0002, CNRS FRE 2500
Neurophysiologie et Nouvelles Microscopies
Paris, France

Oliver Mongin
Mireille Blanchard-Desce
Université de Rennes I
CNRS UMR 6510
Synthèse et Electrosynthèse Organiques
Rennes, France

Jerome Mertz
ESPCI
INSERM EPI 0002, CNRS FRE 2500
Neurophysiologie et Nouvelles Microscopies
Paris, France
E-mail: jerome.mertz@espci.fr

Abstract. We characterize the transmembrane voltage response of a novel second-harmonic generation (SHG) marker using a screening protocol with giant unilamellar vesicles. Two mechanisms are found to contribute to the voltage response: (1) an electro-optic-induced alteration of the molecular hyperpolarizability and (2) an electric-field-induced alteration of the degree of molecular alignment. We quantify the relative weights and of these contributions and provide an upper limit to their response time, which is found to be submillisecond. The identification of two voltage response mechanisms leads to new strategies for the molecular design of membrane potential markers. © *2003 Society of Photo-Optical Instrumentation Engineers.* [DOI: 10.1117/1.1581871]

Keywords: second-harmonic generation; voltage sensing; nonlinear microscopy.

Paper MM-12 received Mar. 6, 2003; accepted for publication Mar. 24, 2003.

Second-harmonic generation (SHG) microscopy is a candidate technique for imaging cellular membrane potential.[1] This technique is based on the use of extrinsic membrane markers that are both hyperpolarizable and amphiphilic.[1–6] Molecular hyperpolarizability ensures that the markers individually produce hyper-Rayleigh scattering, while amphiphilicity ensures that they are distributed in a membrane with a well-defined alignment, enabling a coherent summation of hyper-Rayleigh scattering that leads[7,8] to SHG. Various reports have suggested that SHG imaging can be highly sensitive to a transmembrane electric field,[1–6] more sensitive even than well-established techniques based on fluorescence electrochromism. Currently, the design strategies to improve the SHG electric-field sensitivity have largely concentrated on optimizing the electro-optic response of molecular hyperpolarizabilities.[5,6] A simple two-level model describing molecular hyperpolarizability and the parameters governing its electric field response are presented in Ref. 9. However, an electro-optic mechanism based on changes in molecular hyperpolarizability is not the only mechanism that can lead to SHG membrane potential sensitivity. In particular, an electric-field-induced alteration of the degree of alignment of the membrane markers will also change the SHG power and lead to an apparent membrane potential sensitivity. These two mechanisms, based, respectively, on internal and external molecular degrees of freedom, must be fully characterized to enable quantitative membrane potential imaging. In Ref. 9, we presented an experimental screening protocol that unambiguously distinguishes between the two mechanisms, based on the use of artificial membranes. Reference 9 dealt only with molecules whose response mechanism was identified to be purely electro-optic, and exhibited up to 10 to 20% variations in SHG power for a 100-mV transmembrane voltage. In this paper, we generalize the results of Ref. 9 by examining a molecule whose response mechanism is found to be both electro-optic and realignment in origin. Our goal is to demonstrate that more than one mechanism can contribute to the SHG response, and that care must be taken in properly defining electric field sensitivities. An identification and characterization of these mechanisms leads to new design strategies for optimizing the performance of SHG membrane potential sensors.

We consider the stilbazolium dye molecule, 4-[(1*E*)-2-[4-(dihexylamino)phenyl]ethenyl]-1-(4-sulfobutyl) quinolinium inner salt, illustrated in Fig. 1 and designated as di-6-APEQBS according to Ref. 10. This molecule is push-pull in nature, and hence similar to molecules used in previous reports on SHG membrane imaging. Our experimental protocol to quantify SHG membrane potential sensitivity is described in Ref. 9. We use giant unilamellar vesicles (GUVs) as model bilayer membranes, which are electroformed from a dioleolylphosphatidylcholine (DOPC) deposition. The GUVs are typically 20 to 50 μm in diameter, reside in a 300-mM glucose solution, and are externally labeled with a 5 to 10-μM concentration of di-6-APEQBS. Because of its amphiphilic nature, di-6-APEQBS molecules label only the outer leaflets of the GUVs with a preferred alignment roughly perpendicular to the membrane plane (we will show later that this alignment is far from perfect). Our imaging configuration is that of a scanning laser microscope. A mode-locked Ti:sapphire laser beam (wavelength, 830 nm; repetition rate, 80 MHz) is focused with a 0.9-numerical-aperture (NA) water immersion objective, and scanned through the sample using galvanometer-driven mirrors. The SHG signal is collected in the forward direction with a standard condenser, spectrally selected with bandpass and high-pass optical filters that block both the transmitted laser beam and concurrent two-photon excited fluorescence, and detected with a bialkali cathode photomultiplier tube. Static electric potentials are applied

1083-3668/2003/$15.00 © 2003 SPIE

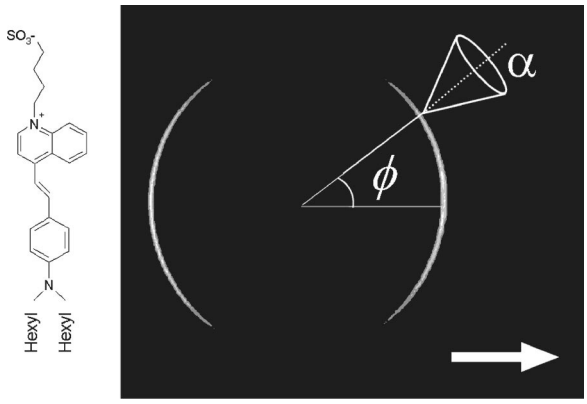

Fig. 1 $SHG_{\parallel}$ image (right) of GUV labeled with di-6-APEQBS (left). Illumination and detection polarizations are directed along the arrow.

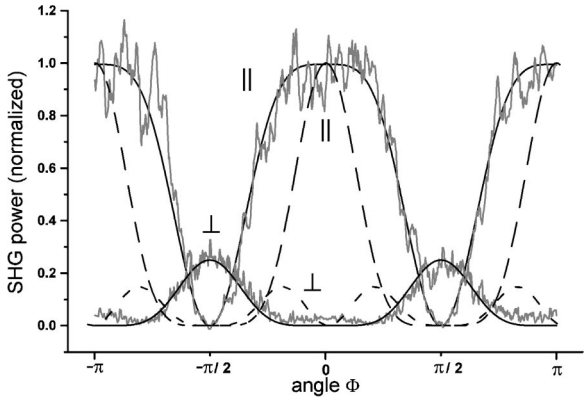

Fig. 2 Observed SHG profiles along GUV equator for parallel (||) and cross (⊥) polarization configurations, along with theoretical fits (solid traces) according to Eq. (1) ($\langle\xi^3\rangle/\langle\xi\rangle=0.5$). The dashed traces represent the predicted profiles if the markers were aligned exactly perpendicularly to the membrane ($\langle\xi^3\rangle=\langle\xi\rangle=1$).

across the GUVs using two platinum bath electrodes separated by about 1.5 cm, which produce[9] transmembrane fields as great as 10^8 V/m. To prevent GUV migration due to electrophoretic forces, we switch the sign of the applied electric field at every new line scan. Odd and even lines of an image then correspond to opposing directions of the applied transmembrane potential.

The emitted SHG power depends both on the tilt angle α of the chromophore axis and on the angle ϕ of the laser beam polarization (linear) with respect to the membrane normal. This is given by

$$\mathrm{SHG}_{\parallel}=\mathrm{SHG}_0(\langle\xi^3\rangle\cos^3\phi+\tfrac{3}{2}\langle\xi-\xi^3\rangle\cos\phi\sin^2\phi)^2$$

$$\mathrm{SHG}_{\perp}=\mathrm{SHG}_0[\langle\xi^3\rangle\cos^2\phi\sin\phi+\tfrac{1}{2}\langle\xi-\xi^3\rangle\times\sin\phi(1-3\cos^2\phi)]^2, \quad (1)$$

where $\mathrm{SHG}_{\parallel,\perp}$ are the signal components, respectively, parallel and perpendicular to the laser beam polarization; and we define $\xi=\cos\alpha$, where $\langle ...\rangle$ denotes an ensemble average over the illuminated chromophore population. Because our vesicles are spherical, the angle ϕ is simply the angular coordinate along a vesicle equator. From Fig. 2, we observe that di-6-APEQBS is not rigorously aligned perpendicularly to the membrane, but instead exhibits a tilt angle distribution such that $\langle\xi^3\rangle/\langle\xi\rangle\approx0.4$ to 0.5. Assuming this distribution is peaked around a fixed tilt angle $\overline{\alpha}$, we conclude $\overline{\alpha}\approx45$ to 50 deg, which is somewhat larger than the tilt angles exhibited by previously studied molecules.[9]

To quantify the SHG membrane potential response of di-6-APEQBS, we applied the alternating voltage between our electrodes and recorded the $\mathrm{SHG}_{\parallel}$ signal generated along the equator of a freshly labeled GUV. Figure 3 illustrates the signal obtained after de-interlacing the GUV image such that $-\pi/2<\phi<\pi/2$ corresponds to an outgoing field and $\pi/2<\phi<3\pi/2$ corresponds to an ingoing field, relative to the vesicle interior. As described in Ref. 9, a purely electro-optic SHG response would lead to the replacement in Eq. (1):

$$\mathrm{SHG}_0\rightarrow\mathrm{SHG}_0(1+\kappa_\beta\xi E_0\cos\phi), \quad (2)$$

where $E_0\cos\phi$ is the applied transmembrane field, and $\kappa_\beta=2\,\mathrm{Re}(\gamma/\beta)$ characterizes the electro-optic response of the molecular hyperpolarizability (β and γ are the first and second hyperpolarizabilities, respectively; we use the notation in Ref. 11). It is apparent from Fig. 3 that an electro-optic response cannot by itself explain the observed variations in the $\mathrm{SHG}_{\parallel}$ profile. In particular, it cannot explain the splitting of the peak response when $-\pi/2<\phi<\pi/2$, nor the narrowness of the peak response when $\pi/2<\phi<3\pi/2$. To properly explain both these features, we must invoke an electric-field-induced alteration of the molecular tilt angle. We characterize this tilt-angle response with the parameter κ_α, such that

$$\xi\rightarrow\xi\left(1+\frac{\kappa_\alpha}{6}E_0\cos\phi\right). \quad (3)$$

Inserting the substitutions of Eqs. (2) and (3) in Eq. (1), and fitting this to the observed $\mathrm{SHG}_{\parallel}$ profile in Fig. 3, we conclude that for di-6-APEQBS in a DOPC membrane at room temperature, then $\kappa_\alpha\approx-4.3\times10^{-9}$ m/V and $\kappa_\beta\approx1.3$

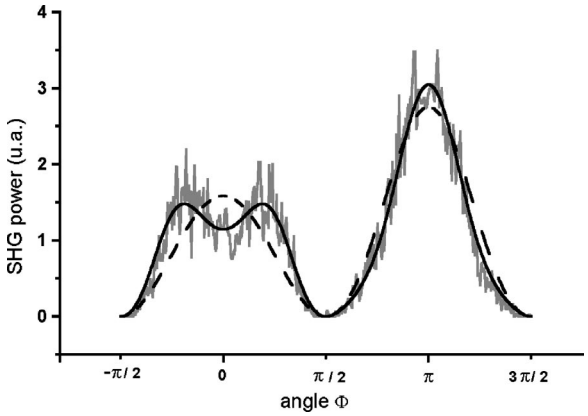

Fig. 3 Observed $\mathrm{SHG}_{\parallel}$ profile along GUV equator during application of 400 mV (at $\phi=0$) transmembrane voltage. Profile is taken from a deinterlaced image such that potential is directed outward for $-\pi/2<\phi<\pi/2$ and inward for $\pi/2<\phi<3\pi/2$. The dashed line corresponds to best fit assuming an electro-optic response mechanism only. The solid line corresponds to best fit when tilt-angle response mechanism is taken into account.

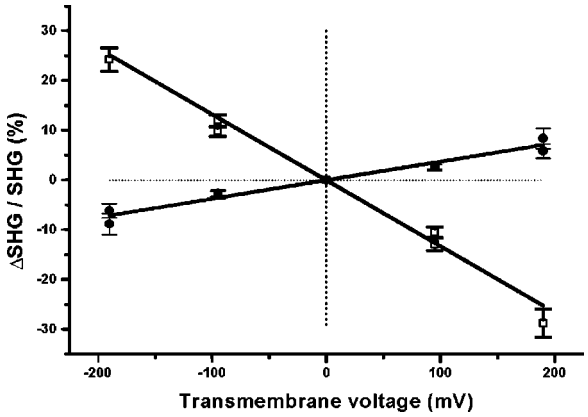

Fig. 4 Relative contributions of electro-optic (bullets) and tilt-angle (open squares) mechanisms to the SHG membrane potential response, as determined from independent SHG profile fits for different applied transmembrane potentials and two different GUVs.

$\times 10^{-9}$ m/V (corresponding, respectively, to -13 and 4% relative SHG changes for a 100-mV transmembrane voltage). The difference in signs between these two parameters indicates that the mechanisms respond in opposing directions.

For membrane potential sensors to be useful in biological applications, they must respond with well-defined sensitivity and adequate speed, independently of the details of the mechanisms involved. In practice, one usually measures the relative change in $\mathrm{SHG}_{\parallel}$ in response to a transmembrane field when the laser polarization is directed perpendicular to the membrane ($\phi = 0$). This is given by

$$\frac{\Delta \mathrm{SHG}_{\parallel}}{\mathrm{SHG}_{\parallel}} = (\kappa_{\alpha} + \kappa_{\beta}) E_0 . \tag{4}$$

Note that, by itself, this measurement cannot reveal the presence of more than one membrane potential response mechanism. Using our protocol, which provides the full angular dependence of the SHG response, we not only identified the presence of both electro-optic and tilt-angle mechanisms, but also determined their relative weights. We verified that these contributions were independently linear, as suggested by Eq. (4), by verifying with independent fits that κ_{α} and κ_{β} remained approximately constant over a wide range of applied transmembrane fields that easily covered the range found in live cells. The results of our verification are shown in Fig. 4, indicating that even though two mechanisms are involved in the SHG response of di-6-APEQBS, the full membrane potential sensitivity remains well defined.

To observe membrane potential variations in excitable cells, adequate SHG response times should be in the submillisecond range. Electro-optic mechanisms are effectively instantaneous on this time scale, since they involve only intramolecular electronic dynamics. On the other hand, tilt-angle mechanisms, which involve global molecular rearrangements, could conceivably be slow on this time scale. As presented, our protocol entailed imaging a small section of membrane and switching the direction of the applied electrode voltage in synchrony with the line-scan period. By changing both the image size and the scan rate, we varied the line-scan period from 20 to 1 ms, the minimum tolerated by our galvanometers, and observed no change in the SHG response amplitude, indicating that the tilt-angle response time was at least as fast as 1 ms. To further refine our temporal resolution, we used asynchronous switching such that the direction of the applied voltage was switched at times separated by intervals 2.5% longer than the line-scan period (Fig. 5). After image deinterlacing, this led to an apparent sliding of the switching time for each successive image line, with a temporal lag step corresponding to 5% of our line-scan period, that is, to 50 μs. Given that the observed membrane width occupied about 15% of our image width, and that about three successive image lines were required for the completion of the SHG response to a voltage switch, we conclude that the tilt-angle response time was at least as fast as 150 μs. Such a response time is entirely adequate for monitoring even fast-voltage transients in cell membranes.

We conclude that, for certain amphiphilic markers, an electro-optic response is not the only mechanism governing SHG membrane potential sensitivity. In particular, our screening protocol revealed that both electro-optic and tilt-angle

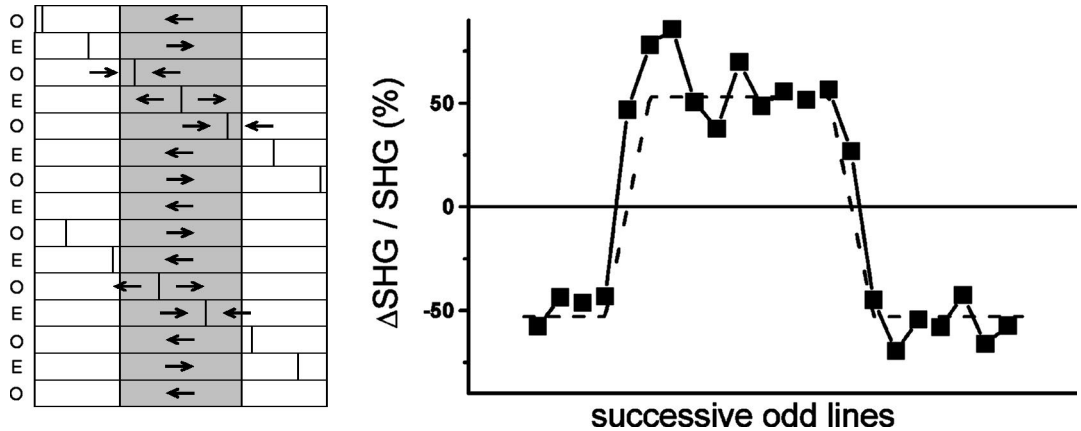

Fig. 5 Asynchronous voltage switching provides better temporal resolution than the line-scan period. (Left) Schematic representation of protocol: image of a small section of membrane (gray) contains odd (O) and even (E) lines. Arrows denote directions of applied 450-mV transmembrane voltage, whose switching period is slightly longer than the line-scan period. When image is deinterlaced (odd lines only), field is initially directed left, then right, then left again. (Right) Observed SHG response following protocol with 1-ms line-scan period and 1.025-ms voltage switching period. Tilt-angle response time is at least as fast as 150 μs. The dashed curve corresponds to the SHG profile if the response were instantaneous.

mechanisms are involved in the SHG response of di-6-APEQBS. Tilt-angle alteration not only undermines the electro-optic response of di-6-APEQBS, but in fact outweighs it significantly. The tilt-angle sensitivity and response time are found to be suitable for biological imaging applications, indicating that tilt-angle mechanisms should not be overlooked when designing SHG membrane potential sensors. In particular, strategies where tilt-angle and electro-optic mechanisms are designed to operate in tandem, rather than in opposition, should lead to exceptionally high performance SHG membrane potential sensors.

Acknowledgments

We are grateful to the CNRS for financial support (ACO and PCV grants). M. Blanchard-Desce acknowledges financial support for young investigators from CNRS (ATIP program). We thank J. Vallée for technical assistance in the synthesis of di-6-APEQBS.

References

1. O. Bouevitch, A. Lewis, I. Pinevsky, J. P. Wuskell, and L. M. Loew, ''Probing membrane potential with nonlinear optics,'' *Biophys. J.* **65**, 672–679 (1993).
2. P. J. Campagnola, M. Wei, A. Lewis, and L. M. Loew, ''High-resolution nonlinear optical imaging of live cells by second harmonic generation,'' *Biophys. J.* **77**, 3341–3349 (1999).
3. G. Peleg, A. Lewis, M. Linial, and L. M. Loew, ''Non-linear optical measurement of membrane potential around single molecules at selected cellular sites,'' *Proc. Natl. Acad. Sci. U.S.A.* **96**, 6700–6704 (1999).
4. D. Gross, L. M. Loew, and W. W. Webb, ''Optical imaging of cell membrane potential changes induced by applied electric fields,'' *Biophys. J.* **50**, 339–348 (1986).
5. V. Alain, M. Blanchard-Desce, I. Ledoux-Rak, and J. Zyss, ''Amphiphilic polyenic push-pull chromophores for nonlinear optical applications,'' *Chem. Commun.* **5**, 353–354 (2000).
6. L. Porrès, O. Mongin, B. K. G. Bhatthula, M. Blanchard-Desce, L. Ventelon, L. Moreaux, T. Pons, and J. Mertz, ''Molecular probes for two-photon excited fluorescence and second harmonic generation imaging of biological membranes,'' *Proc. SPIE* **4812**, 24–33 (2002).
7. L. Moreaux, O. Sandre, and J. Mertz, ''Membrane imaging by second-harmonic generation microscopy,'' *J. Opt. Soc. Am. B* **17**(10), 1685–1694 (2000).
8. L. Moreaux, O. Sandre, S. Charpak, M. Blanchard-Desce, and J. Mertz, ''Coherent scattering in multi-harmonic light microscopy,'' *Biophys. J.* **80**(3), 1568–1574 (2001).
9. L. Moreaux, T. Pons, V. Dambrin, M. Blanchard-Desce, and J. Mertz, ''Electro-optic response of second-harmonic generation membrane potential sensors,'' *Opt. Lett.* **28**, 625–627 (2003).
10. L. M. Loew, ''Potentiometric dyes: imaging electrical activity of cell membranes,'' *Pure Appl. Chem.* **68**(7), 1405–1409 (1996).
11. P. N. Butcher and D. Cotter, *The Elements of Nonlinear Optics*, Cambridge University Press, Cambridge (1990).